

Rhythmic changes in spike coding in the rat suprachiasmatic nucleus

G. S. Bhumbra, A. N. Inyushkin, K. Saeb-Parsy, A. Hon and R. E. J. Dyball

Department of Anatomy, University of Cambridge, Downing Street, Cambridge CB2 3DY, UK

The suprachiasmatic nucleus is regarded as the main mammalian circadian pacemaker but evidence for rhythmic firing of single units *in vivo* has been obtained only recently. The present study was undertaken to determine if rhythms could be seen using measures of activity in addition to the mean spike frequency. We investigated whether there were changes in the irregularity of cell activity measured by the disorder of the interspike interval distribution for neurones recorded *in vivo* and *in vitro*. By plotting the entropy of the log interval histogram that quantifies the coding capacity for each action potential against the respective zeitgeber time, we describe oscillations of spike activity *in vivo*. Entropy measures have the advantage over variances in that they quantify aspects of the shape of the distribution and not just the dispersion. One hundred and sixty-six cell recordings from the suprachiasmatic nucleus showed a significant rhythm in entropy with an oscillatory trend in the data ($P < 0.001$) showing a trough towards the end of the light period and a peak in the mid-dark period. There was a similar rhythm for the cells recorded from the peripheral zone ($n = 209$, $P = 0.037$). In separate experiments *in vitro*, to investigate the relationship between mean spike frequency and entropy, potassium-induced depolarization of cells recorded during the subjective night was correlated with a significant increase in mean spike frequency ($r = 0.259$, $P = 0.011$) and a decrease in entropy ($r = -0.296$, $P = 0.004$). The negative correlation between the entropy and mean spike frequency of cells recorded *in vitro* was significantly different from that seen *in vivo* ($F = 15.5$, $P < 0.001$), which may reflect differences in the balance between deterministic and stochastic influences on spike occurrence. The study shows that while there is a rhythm of mean spike frequency, parameters based on the variability of interspike interval distributions also display rhythmic changes over the day–night cycle.

(Resubmitted 23 November 2004; accepted after revision 16 December 2004; first published online 20 December 2004)

Corresponding author R. E. J. Dyball: Department of Anatomy, University of Cambridge, Downing Street, Cambridge CB2 3DY, UK. Email: red1000@cam.ac.uk

The cyclic nature of neural activity in the suprachiasmatic nucleus has been known for some time as a result of electrophysiological recordings made over the day–night cycle. Recordings of single unit activity *in vitro* exhibit rhythmic changes, suggesting that cyclicality is preserved in the slice preparation (Green & Gillette, 1982; Shibata *et al.* 1982; Groos & Hendriks, 1982). The term ‘rhythm’ in this context is used to describe any feature of activity that is repeated with a regular period. Multiple unit activity shows variation over the day–night cycle both *in vivo* and *in vitro* (Inouye & Kawamura, 1979; Bouskila & Dudek, 1993; Meijer *et al.* 1997). Only recently has evidence been published for a daily rhythm of single unit activity in the suprachiasmatic nucleus *in vivo* (Saeb-Parsy & Dyball, 2003).

Quantifying spontaneous activity

In the past, for both *in vivo* and *in vitro* studies on the suprachiasmatic nucleus, the almost universally adopted

measure of spontaneous ‘activity’ has been mean spike frequency. An alternative approach that might provide information in addition to mean spike frequency is to focus on the intervals between spikes rather than the spikes themselves. The duration of the intervals between spikes can be used to construct an interspike interval histogram that represents the distribution of intervals of different lengths (Gerstein & Mandelbrot, 1964).

An approach based on information theory has been previously developed and applied to the interspike intervals (Bhumbra & Dyball, 2004). Here we characterize the relationship between the information conveyed by spontaneously firing cells and the corresponding zeitgeber time. We define ‘information’ as a mathematical quantity that is synonymous with entropy (Shannon & Weaver, 1949). Both thermodynamic and statistical entropies are measures of disorder, but the statistical entropy used in this paper was defined by Shannon & Weaver (1949) as the minimum descriptive complexity of a random variable.

The entropy of the log interval probability distribution is used as a measure of the irregularity of activity. It quantifies the coding capacity per spike in a way that is separate from and independent of the mean spike frequency (Bhumbra & Dyball, 2004). The term 'code' is used to describe any system that expresses information in a form that may be used for processing or transmission. Oscillatory changes in entropy over the day–night cycle are described using Fourier analysis (Bhumbra *et al.* 2004b). We introduce randomization (Monte-Carlo) methods to test for significance in rhythm in a way that avoids an arbitrary choice of temporal bin width over which to pool the data.

Conventional measures of variability based on variances, such as the standard deviation of the mean spike frequency or the coefficient of variation of the intervals (standard deviation/mean interval), are limited because they measure only the spread of a distribution and not its shape (Jaynes, 2003). Entropy reflects not only the variance but also the skewness, kurtosis, and all other aspects of the profile of a distribution. Many cells of the suprachiasmatic nucleus show a bimodal interval distribution (Saeb-Parsy & Dyball, 2003) that might not remain constant. Unlike variance measures, the entropy of the log interval probability distribution is sensitive to changes from a unimodal to a bimodal distribution of intervals. This means a change in modality that would affect the entropy might not be detected using variance measures only.

The rhythmic activities from the core and peripheral regions of the suprachiasmatic nucleus are compared. A comparison is also made between those cells with caudal projections towards the region of the arcuate nucleus and those without. To investigate the possibility that the changes in the depolarized state of the neurones may explain the diurnal variations in activity, we apply an information approach to recordings of suprachiasmatic cells made *in vitro* where potassium levels were modified to depolarize the cells.

Methods

Male Wistar rats, provided with food and water *ad libitum*, were used for both *in vivo* and *in vitro* experiments. All experiments were carried out in accordance with the Animals (Scientific Procedures) Act (UK) 1986.

Recordings *in vivo*

Rats weighing between 250 and 300 g were used for recordings *in vivo* and housed under a 12 h light–12 h dark regime for at least 14 days before each experiment. Animals were anaesthetized with urethane at a dose of 1.1 g kg⁻¹ i.p. The jugular vein was cannulated and a tracheostomy was performed. Using the ventral surgical approach (Leng &

Dyball, 1991), the suprachiasmatic nucleus and arcuate nucleus were exposed (Saeb-Parsy & Dyball, 2003). A bipolar stimulating electrode was lowered into the region of the arcuate nucleus. Extracellular recordings from the suprachiasmatic nucleus region were made using glass electrodes with a tip diameter of approximately 0.5 μm filled with 2% pontamine sky blue in 0.5 M sodium acetate to give a tip of resistance 5–15 M Ω . Recorded signals were preamplified then filtered using a 50 Hz noise eliminator (Hum Bug; Quest Scientific, North Vancouver, Canada). The signal was then amplified and passed through an interface device (1401 Plus; Cambridge Electronic Design, Cambridge, UK) to a computer. Spike2 (Cambridge Electronic Design) software was used to collect the data.

An online hardware discriminator (Digitimer D130) was used to detect spikes. Randomised simulations of misdiscrimination showed no consistent effect of misdiscrimination on the entropy values since it was dependent on the type of spike activity. For a cell with doublet motifs, typical of those of the suprachiasmatic nucleus *in vivo*, the entropy remained within 99% of its true value after randomly excluding 20% of the spikes whereas an addition of 1% of false triggers was sufficient to affect the entropy beyond this limit. Recordings were thus excluded if interspike intervals of less than 2 ms suggested the presence of false triggers. Cells were recorded for a minimum of 10 min and five spikes. A low minimum for the number of spikes recorded was selected to avoid biasing the data against virtually silent cells. The minimum duration of the excerpt was chosen to allow us to satisfy ourselves that the firing in the selected epoch was stable. During long recordings from the same cell, excerpts of spontaneous activity used for data analysis were separated by at least 1 h. This period of separation was chosen so that enough spikes could be recorded to obtain a satisfactory log interval histogram from very slow firing cells. Neurones were continuously recorded until they were either lost or when spike discrimination became unreliable. Recordings were rejected if the spike height became too small (when the maximum spike amplitude was less than twice that of the range of the noise). Since recordings were monitored continually, slow changes from one cell to another were easily seen. The experimental design involved recording from single cells for a period of time sufficient to obtain a satisfactory profile for the interspike interval distribution at different zeitgeber times. An across-population analysis was then undertaken to test for rhythmicity. This approach was adopted rather than recording single units for more than 24 h because such recordings are not technically feasible *in vivo*.

All cells were tested to determine whether they had caudal projections to the region of the arcuate nucleus by antidromic activation, confirmed using a two-shock collision test (Saeb-Parsy *et al.* 2000). Anatomically, cells were localized with reference to the position of the

recording electrode at the end of each experiment, marked by depositing pontamine blue from its tip with a direct current of 5–10 mA for approximately 10 min. Only one electrode was used for a single track in each animal so that cells recorded by each electrode could be located accurately with reference to the final position of the electrode tip. At the end of each experiment, the rat was fixed by perfusion of the brain via the heart using 10% formaldehyde in isotonic saline. A microtome was used to cut 50 μm sections and microscopic inspection of the slices was undertaken to locate the blue spot and so reconstruct the sites of recordings for every cell in each animal.

Histological reconstruction of electrode position *in vivo*

The positions of all the neurones in the region of the suprachiasmatic nucleus were determined by the method of histological reconstruction (Saeb-Parsy & Dyball, 2003). Neurones within the cell-dense central region were differentiated from those in the peripheral zone of the suprachiasmatic nucleus. The central region

was defined by a perimeter 500 μm distant from the centre of the central region of the SCN on the side from which recordings were made. The peripheral zone included a region 500 μm further from the centre of the nucleus (Fig. 1). Any cell beyond the peripheral zone was regarded as outside the nucleus and excluded from subsequent analysis (see below). Lesion studies based on the ablation of the suprachiasmatic nucleus to abolish rhythms of activity (Moore & Eichler, 1972; Stephan & Zucker, 1972) did not strictly define the precise limits of the region of the nucleus. For the present study, the cells of the central region would have included most of the neurones described by intrinsic circuitry studies (Leak *et al.* 1999) as within both core and shell regions of the suprachiasmatic nucleus.

During the course of the recording *in vivo* it was difficult to be sure that the electrode was correctly located and some cells were recorded from near as well as within the suprachiasmatic nucleus. It thus became necessary to exclude some recordings but it was argued that inclusion of inappropriate cells, which showed no rhythmic activity, could not have imposed an artefactual rhythm on the whole population of recorded cells that did show a rhythm.

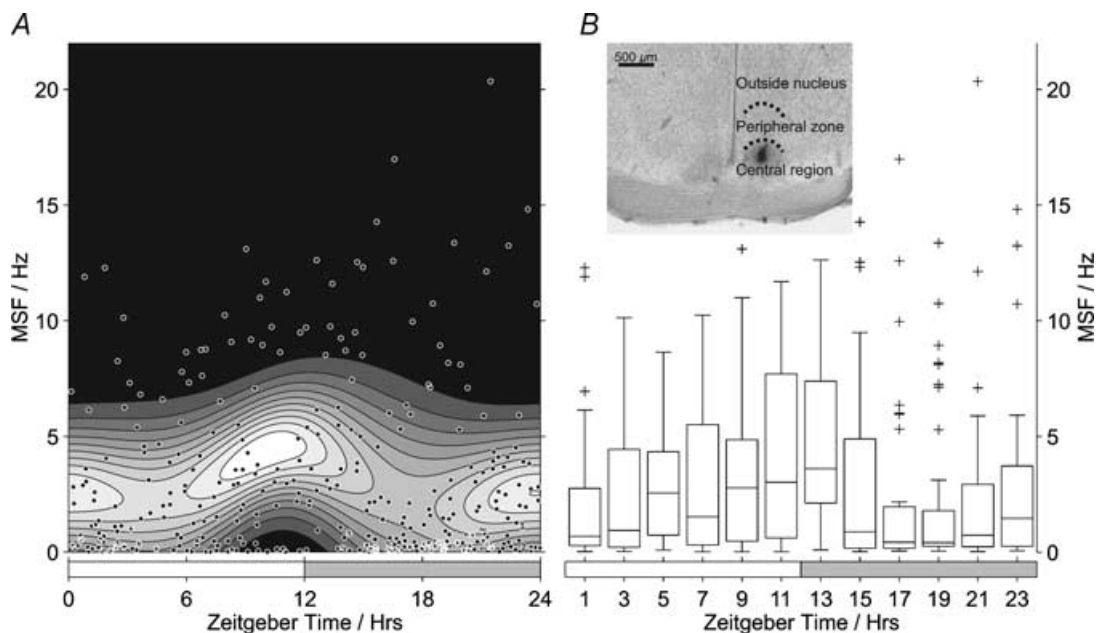


Figure 1. The mean spike frequency (MSF) of cells recorded from the suprachiasmatic nucleus *in vivo* showed a day-night rhythm

Parametric (A) and non-parametric (B) representations of the data are shown. A, a contour plot modelling the conditional probability of mean spike frequency given the zeitgeber time, based on the best-fits for the mean and standard deviation of the data, with a lighter shading indicating a region of increased probability and the raw data overlaid as circular points. The contour plot represents a range of probability density from 0 (black) to the maximum value (white), using 10 intermediate contour divisions; for this contour plot, the maximum probability density is 0.244. B, box-and-whiskers plot for the mean spike frequencies using twelve 2 h bins. (A box-and-whiskers plot represents the median as a single line with a box to indicate the interquartile range; the whiskers represent the furthest data values within 1.5 times the interquartile range away from the lower and upper quartile, and outliers are marked as crosses.) A Kruskal-Wallis one-way ANOVA showed a significant difference in activity for at least a single 2 h epoch ($\chi^2 = 24.3$, $P = 0.012$). The inset indicates the positions of the central and peripheral regions of the suprachiasmatic nucleus from where cells, represented in the figure, were recorded.

The decision was thus made to investigate the rhythmic activity of the cells in the central region and peripheral zone treated both as a single combined group and as separate groups. It seemed impossible that the inclusion of inappropriate cells could have imposed an artefactual rhythm. It was argued that inclusion of inappropriate cells could have only 'diluted' the rhythm. Despite their inclusion a highly significant rhythm was seen.

Spike analysis *in vivo*

For each recording, the mean spike frequency and the mean of the log intervals were determined and the corresponding zeitgeber time was taken from the middle of the recording period. Subsequent spike analysis was undertaken as previously described (Bhumbra & Dyball, 2004) for the single cell recordings at the different zeitgeber times before undertaking an across-population analysis to test for rhythmicity. Briefly, to measure spike irregularity, an information approach was adopted to quantify the entropy of the probability distribution of the intervals on a logarithmic scale. A log interval histogram of a bin width $0.02 \log_e$ (time) was convolved with a Gaussian kernel with a standard deviation one-sixth of that of the log data x_i . By normalizing the histogram, a probability mass distribution $P(x_i)$ was constructed to calculate the log interval entropy $S(X)$ using Shannon's equation (Shannon & Weaver, 1949).

$$S(X) = - \sum_{i=1}^{N_X} P(x_i) \log_2 P(x_i) \quad (1)$$

where N_X is the number of bins in $P(x_i)$.

The best-fit for the log interval entropy of the cells was obtained using the least-squares Levenberg-Marquardt iterative algorithm (Wadsworth, 1990) to converge to optimal values for the Fourier coefficients for a function $f(t)$ expressed with respect to an offset term a_0 and Fourier coefficients a_j and b_j .

$$f(t) = \frac{a_0}{2} + \sum_{j=1}^{\nu} \left(a_j \cos \frac{2\pi j}{T} t + b_j \sin \frac{2\pi j}{T} t \right) \quad (2)$$

where t is the fractional zeitgeber time over the period T and ν is the harmonic order.

A second order harmonic expansion was used to fit the data ($\nu = 2$), and the range of the fit was used as a measure of the amplitude of the rhythm. To test for significance of rhythm, a randomization (Monte-Carlo) approach was adopted, in which an identical fitting algorithm was applied to the same data after randomly reassigning the original zeitgeber times to the data values to remove any underlying rhythmicity. The range of the fit for the randomised data was determined as a measure of rhythm amplitude, and the procedure was repeated 10 000 times in total. Each P -value, for the chance that the data showed no

cyclicality, was obtained from the proportion of amplitudes calculated from the randomised data that exceeded that of the observed data.

Influence of ambient light *in vivo*

During the entire period of preparation and recording *in vivo*, illumination was maintained above a level of 260 lux at all times. This was done to avoid variability between experiments. Fluorescent tube lighting in the rooms used to house the animals during the light period produced light of an intensity of 260 lux. The fluorescent tubes used in the laboratory used for recording were of identical specification with respect to wavelength composition. However, the light intensity was always greater than 260 lux during recording to prevent any dark effects that might have imposed a rhythm.

It would have been impossible to carry out the preparative surgery in the dark. The time required for the surgery and before the first recordable cell was encountered was variable (1–2 h). It would have been possible to record in the dark after this time but the period of light exposure and its timing would have varied between experiments. To avoid such variability, light was maintained constant. Maintaining a constant light is unlikely to have imposed an artefactual rhythm. It is possible that it might have attenuated or blurred an existing rhythm. Any resetting effect cannot have been sufficient to disrupt the rhythm completely, however, because, despite any possible effects of constant light, a highly significant rhythm was seen.

Recording *in vitro*

Rats weighing between 75 and 150 g were used for recordings *in vitro* and housed under a 12 h light–12 h dark regime for at least 7 days before each experiment. Animals were anaesthetized with urethane at a dose of 1.1 g kg^{-1} i.p. Following decapitation, the brains were excised, and a Vibratome (Series 1000; Horwell Instruments, St Louis, MO, USA) was used to cut sagittal slices of thickness $500 \mu\text{m}$ through the suprachiasmatic nucleus. Slices were transferred to the recording chamber and perfused with artificial cerebrospinal fluid (aCSF) oxygenated with 95% oxygen and 5% carbon dioxide. The composition of the aCSF was (mM): NaCl 124, KCl 3, KH_2PO_4 1.24, CaCl_2 2.1, MgSO_4 1.3, NaHCO_3 24, and glucose 10 (Cui *et al.* 1997). The recording chamber was maintained at 32.8°C . Extracellular recordings were made using glass electrodes with a tip diameter of approximately $0.5 \mu\text{m}$, filled with 0.9% NaCl to give a tip resistance of approximately $10 \text{ M}\Omega$. The data acquisition hardware and protocols were identical to those used *in vivo*, except that the minimum time allowed for each recording was 5 min beginning at least 5 min after the start of the recording or after

any change in extracellular potassium concentration to ensure stable conditions. In addition to the hardware discrimination, the raw waveform was sampled at 20 kHz and offline discrimination of spike events was undertaken using custom software (Dyball & Bhumbra, 2003) for subsequent data analysis. After the spontaneous activity of each cell had been recorded in normal aCSE, the neurones were depolarized by increasing the concentration of potassium in the medium solution. The extent of the increase in extracellular potassium $\Delta[K^+]_o$ from the initial concentration $[K^+]_o$ was used to estimate the degree of depolarization ΔE , based on their interrelation given by a formula derived from the Nernst equation (the derivation of the formula is provided in the Appendix):

$$\Delta E = \frac{RT}{F} \log_e \left(1 + \frac{\Delta[K^+]_o}{[K^+]_o} \right) \quad (3)$$

where R is the ideal gas constant ($8.3143 \text{ J mol}^{-1} \text{ K}^{-1}$), T is the absolute temperature (306 K), and F is Faraday's constant (96485 C mol^{-1}).

Cells were depolarized in estimated steps of 3 mV. Spike analysis was undertaken as previously described for the recordings *in vivo*. For each depolarizing increment, the mean spike frequency and the mean of the log intervals were determined. The simple use of the Nernst equation to estimate the changes in membrane potential assumes that the neurilemma is permeable only to potassium ions and not, for example, to sodium or chloride ions. To determine the extent to which the Nernst equation would overestimate the change in membrane potential as a result of only considering potassium ions, the values were compared with those obtained using the Goldman-Hodgkin-Katz equation. The Goldman-Hodgkin-Katz equation does take into account the influence of sodium and chloride ions on the membrane but requires estimates of the intracellular concentrations of the ions and their relative conductances. To our knowledge, such estimates are not available for suprachiasmatic cells so we used standard values (Purves *et al.* 2001) for the intracellular concentrations ($[K^+]_i = 140 \text{ mM}$, $[Na^+]_i = 10 \text{ mM}$, $[Cl^-]_i = 10 \text{ mM}$) and relative conductances ($g_K : g_{Na} : g_{Cl} = 25 : 1 : 10$). The result of eqn (3) would at most overestimate the change in membrane potential by double the value obtained using the Goldman-Hodgkin-Katz equation.

The estimate obtained by eqn (3) was used to give some indication of the extent of depolarization. The use of the Nernst equation on its own rather than the Goldman-Hodgkin-Katz equation was simpler and avoided any need to estimate the intracellular concentrations of the ions or of their conductances that may not have been constant at different levels of depolarization. To confirm our estimates of the changes in membrane potential that occurred with each addition

of potassium, we made a short series of whole-cell patch recordings from SCN cells. We recorded with pipettes filled with a solution that contained (mM): potassium gluconate 130, KCl 10, Hepes 10, $MgCl_2$ 2, K_2ATP 2, pH 7.3, and with a resistance of 3–10 M Ω . Whole cell recordings of the membrane potential were made from eight cells during step changes in potassium concentration identical to those used during the extracellular experiments. The estimated depolarization from eqn (3) was plotted against the measured change in membrane potential ($n = 30$). Change in membrane potential was strongly related to the estimated depolarization ($P < 0.001$; $r = 0.721$) with a slope of 0.825. The 95% confidence interval for the slope ranged from 0.450 to 1.200, and a two-tailed t test confirmed that the slope did not significantly differ from 1 ($t = 0.9534$, $P = 0.826$). This suggested that it is justified to use eqn (3) to estimate the change in membrane potential. Furthermore, any systemic inaccuracies in the estimate would not have affected the validity of the analysis. The estimated changes in membrane potential were used only for non-parametric rank test statistics. The only assumption made by such an approach is that an increased extracellular potassium concentration is associated with a depolarization of the membrane and the observations described above show that depolarization did indeed occur. The absolute magnitude of the depolarization would not have affected the rank test statistics.

Results

Altogether, 469 recordings with histological estimation of the cell location were made in the region of the supra-chiasmatic nucleus *in vivo*. The presence of short intervals in 39 recordings required their exclusion, and an additional 55 recordings were made from cells that were located outside the nucleus. For the remaining 375 recordings, a total of 87 h and 51 min of recording of spontaneous activity was collected. One hundred and sixty-six recordings were made from cells in the central region of the nucleus whereas 209 recordings were made from cells in the peripheral zone. From both regions of the supra-chiasmatic nucleus, 158 recordings were obtained during the subjective day-time and 217 during the subjective night-time. Of the 23 cells recorded *in vitro*, the numbers tested for estimated depolarization by 3, 6, 9, 12, 15 and 18 mV were 20, 18, 14, 9, 3 and 7, respectively.

Changes in activity *in vivo*

Consistent with previous findings *in vitro* (Green & Gillette, 1982; Shibata *et al.* 1982; Groos & Hendriks, 1982) and *in vivo* (Saeb-Parsy & Dyball, 2003), a rhythm in mean spike frequency was seen *in vivo* (Fig. 1A). A non-parametric Kruskal-Wallis one-way ANOVA undertaken on the data, divided into 12 groups by the corresponding 2 h bin (Fig. 1B), showed a significant

difference in activity for at least a single 2 h epoch ($\chi^2 = 24.3$, $P = 0.012$). While the activity during the subjective night showed a lower mean spike frequency, there were more outlying points than during the subjective day. However, Fig. 1B shows a reduction in the inter-quartile range at zeitgeber time 17–19 h because of the clustering of very low values during the subjective night.

A plot of the entropy of log intervals against the zeitgeber time showed a scatter with a visible diurnal variation that obviously differed from a similar scatter obtained from the same data values after randomization (see Fig. 2B). A Kruskal-Wallis one-way ANOVA on the entropy data, divided into 12 groups by the corresponding 2 h bin, showed a highly significant variation in activity over the day–night cycle ($\chi^2 = 41.9$, $P < 0.001$). The Monte-Carlo randomization algorithm also confirmed that the raw data showed a significant rhythm ($P < 0.001$).

The rhythmic activity of cells in the central region of the suprachiasmatic nucleus was more obvious than that in the peripheral zone (see Fig. 3). The overall profile for the changes in activity appeared to be similar. In both cases, the entropy of the log interval showed a trough towards the end of the light period, and a peak in the mid-dark period. However, the Monte-Carlo randomization algorithm showed that the existence of rhythmic activity in the central region of the suprachiasmatic

nucleus was somewhat more convincing with a greater level of significance ($P < 0.001$) than that seen in the peripheral zone ($P = 0.037$).

The number of cells that showed outward connections towards the region of the arcuate nucleus, as identified by antidromic stimulation (Saeb-Parsy *et al.* 2000), was 78 whereas 297 did not. Despite the comparatively small number of neurones with the projection, the Monte-Carlo randomization algorithm confirmed a significant ($P = 0.006$) rhythm that suggested the existence of a second peak in the mid-light period (see Fig. 4). The remaining cells not so identified also showed a significant ($P < 0.001$) rhythm but with a trough in the log interval entropy towards the end of the mid-light period.

Since the entropy of the log intervals was calculated in a way that was dependent on the shape of the log interval histogram, rather than on its central location, changes in the mean of the log intervals were investigated. Figure 5 illustrates the changes in the log interval mean. The presence of two similar peaks and two similar troughs is suggestive of a profile that is more complex than a single fundamental cycle. A Monte-Carlo randomization algorithm confirmed a significant ($P = 0.012$) rhythm.

To investigate how the mean spike frequency might relate to the entropy and the log interval mean, scatters were plotted as shown in Fig. 6A and B, respectively.

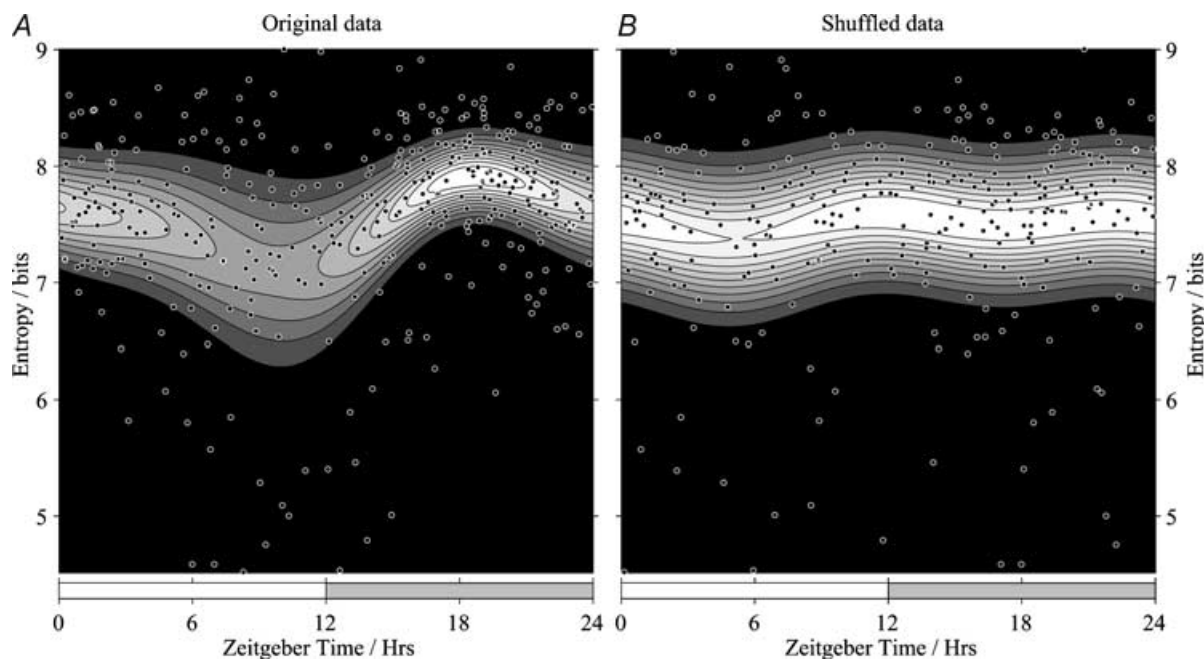


Figure 2. The raw data for the entropy of the log interval distribution show a visible diurnal variation and can be used to assess changes in the activity of cells recorded *in vivo* from the suprachiasmatic nucleus in a numerically sound manner (rhythm significance: $n = 375$, $P < 0.001$)

A, the log interval entropy against the zeitgeber time for each recording, overlaying a contour plot modelling the conditional probability (with a range of 0–2.09, see Fig. 1) of the log interval entropy given the zeitgeber time (see Fig. 1A). B, an equivalent representation (with a range of 0–1.36 in probability density) to illustrate a Monte-Carlo trial in which the original zeitgeber times were randomly reassigned to the data values to remove any underlying rhythmicity.

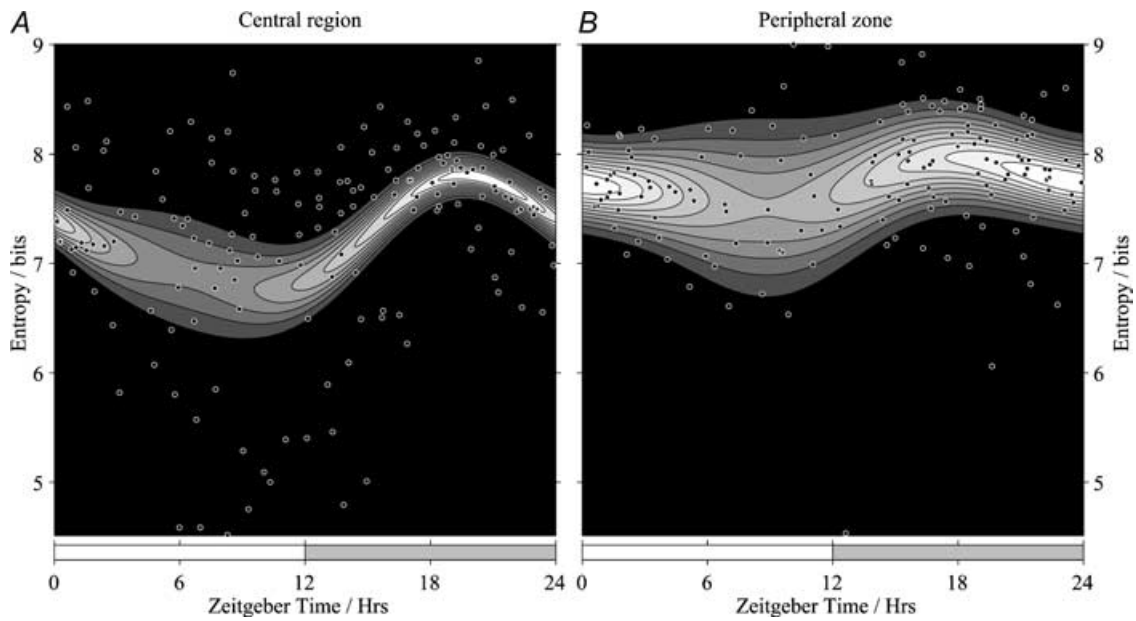


Figure 3. The rhythmic activity of cells in the central region (rhythm significance: $n = 166$, $P < 0.001$) of the suprachiasmatic nucleus is more obvious than that in the peripheral zone (rhythm significance: $n = 209$, $P = 0.037$)

A, a scatter overlaying a contour plot (with a range of 0–4.07 in probability density, see Fig. 1) for cells recorded in the central region of the suprachiasmatic nucleus. *B*, an equivalent plot (with a range of 0–1.91 in probability density) for the cells recorded from the peripheral zone.

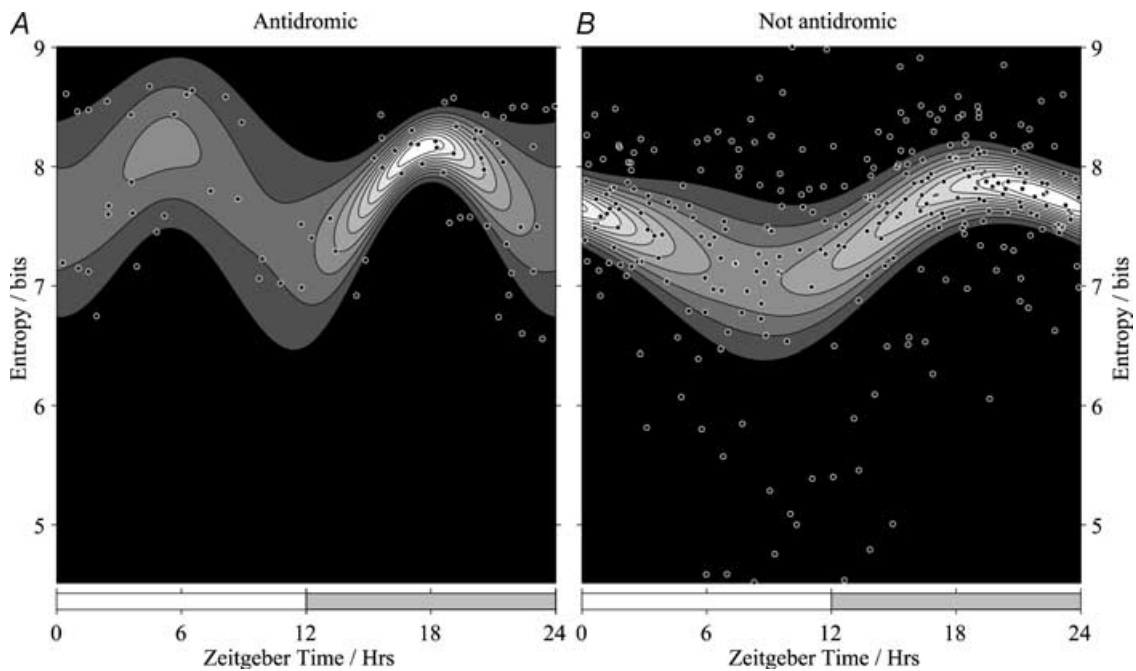


Figure 4. Cells of the suprachiasmatic nucleus with an outward projection towards the region of the arcuate nucleus, identified by antidromic stimulation, show a rhythm (rhythm significance: $n = 78$, $P = 0.006$) in activity that appears to be distinctly biphasic compared to those cells without (rhythm significance: $n = 297$, $P < 0.001$)

A, a scatter overlaying a contour plot (with a range of 0–2.84 in probability density, see Fig. 1) for cells that project towards the region of the arcuate nucleus. *B*, an equivalent plot (with a range of 0–2.82 in probability density) for the cells that do not.

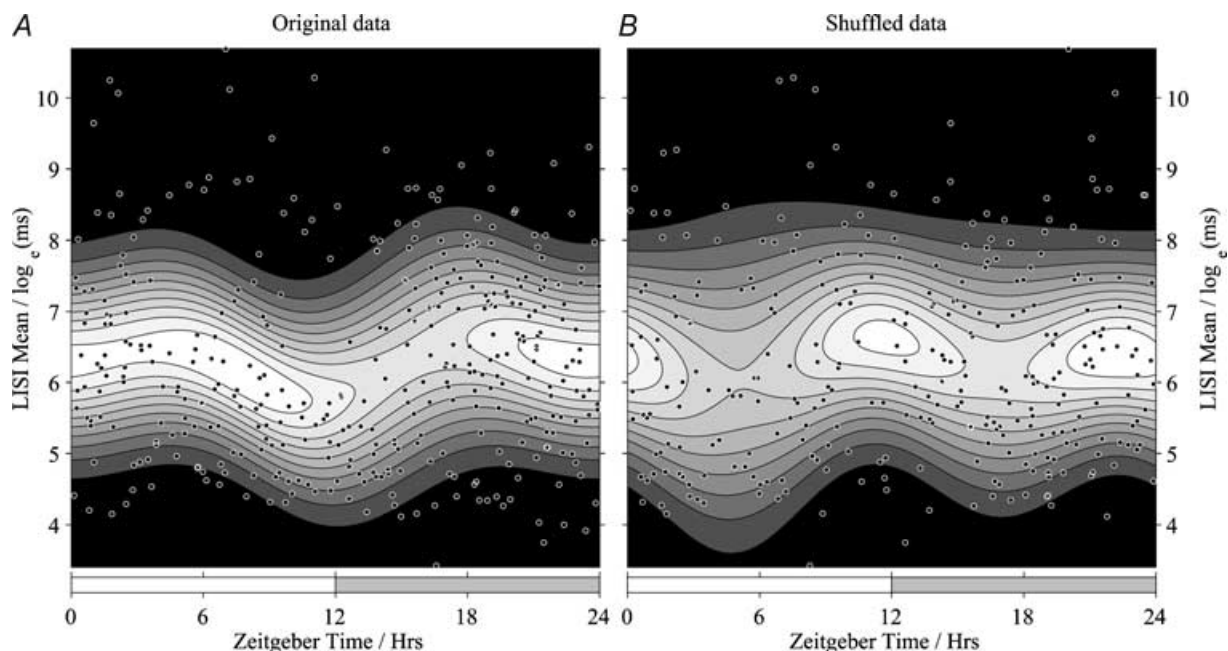


Figure 5. The mean of the log intervals (LISI mean) shows a visible diurnal variation (rhythm significance: $n = 375$, $P = 0.012$)

A, a scatter overlaying a contour plot (with a range of 0–0.549 in probability density, see Fig. 1) for the cells recorded from the central region and peripheral zone of the suprachiasmatic nucleus. *B*, an equivalent representation (with a range of 0–0.584 in probability density) to illustrate a randomised (Monte-Carlo) trial (see Fig. 2*B*).

Pearson's moment correlation statistics were used to test for significant trends with respect to the log of the mean spike frequency. A negative correlation was statistically significant for the entropy ($r = -0.704$, $P < 0.001$) and

the log interval mean showed a very strong negative relationship ($r = -0.965$, $P < 0.001$). A similar analysis was undertaken to characterize how the log interval entropy was associated with the log interval mean and

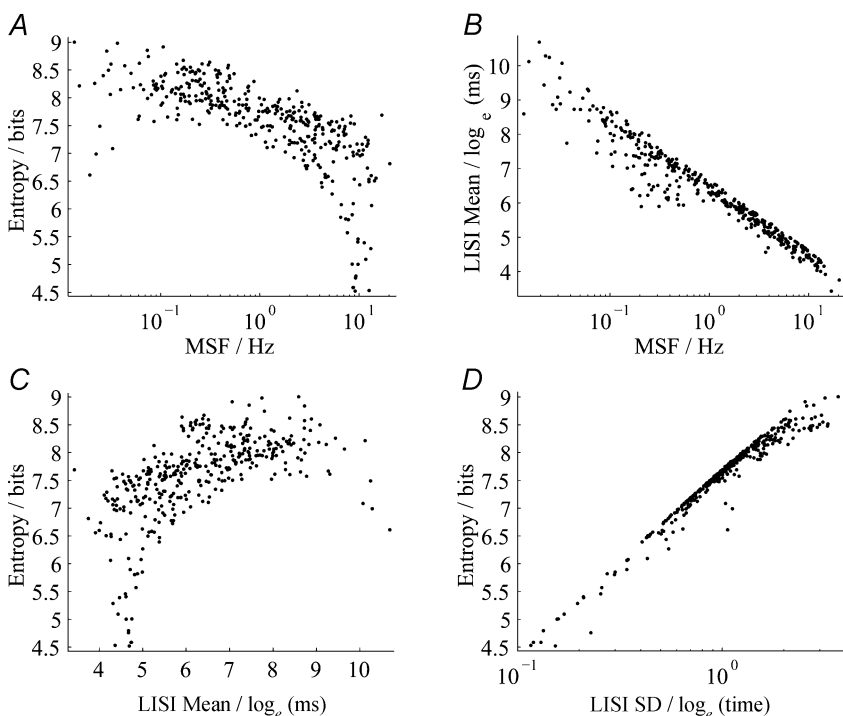


Figure 6. The mean spike frequency and log interval entropy are correlated with other measures of activity of cells recorded *in vivo* from the suprachiasmatic nucleus

The entropy of the log interval distribution (*A*) and the log interval mean (LISI Mean) (*B*) plotted against the mean spike frequency on a log scale. Pearson's moment correlation showed significant correlations with respect to the logarithmic frequency for both the entropy ($r = -0.704$, $P < 0.001$) and log interval mean ($r = -0.965$, $P < 0.001$). The entropy is also plotted against the log interval mean (LISI Mean) (*C*) and the log interval standard deviation (LISI SD) on a log scale (*D*), with positive correlations evident in both cases ($r = 0.579$, $P < 0.001$ and $r = 0.975$, $P < 0.001$, respectively).

standard deviation (see Fig. 6C and D). A positive correlation was statistically significant for the log interval mean ($r=0.579$, $P < 0.001$) and the log standard deviation of the log intervals showed a very strong positive relationship ($r=0.975$, $P < 0.001$).

The trends shown in Fig. 6 could be described by regression fits. If f represents the mean spike frequency and $S(X)$ denotes the entropy of the log intervals, they could be interrelated by $\log_e(f) = -0.324S(X) + 7.57$ and the relationship between the mean μ of the log intervals and the frequency f was given by $\log_e(f) = -0.801\mu + 6.29$. A regression fit for the entropy $S(X)$ with respect to the log interval mean μ could be expressed by the equation $S(X) = 0.321 + 5.55$ and the entropy $S(X)$ and standard deviation of the log intervals σ could be related in a similar way $S(X) = 0.905 \log_2(\sigma) + 7.57$. For the last regression

fit, the 99.9% confidence interval (Wadsworth, 1990) for the slope was 0.869–0.940 and for the intercept, 7.54–7.59.

Effects of depolarization *in vitro*

To investigate how depolarization might affect the relationship between mean spike frequency and entropy, the same parameters were measured for cells recorded *in vitro* subjected to a raised concentration of extracellular potassium that might be expected to cause depolarization. The responses of two representative cells to raised extracellular potassium are shown in Fig. 7, and the corresponding plots for the changes in mean spike frequency and entropy are illustrated in Fig. 8A. In Fig. 7, the probability distributions of the log intervals are shown for each depolarization step. Each probability distribution

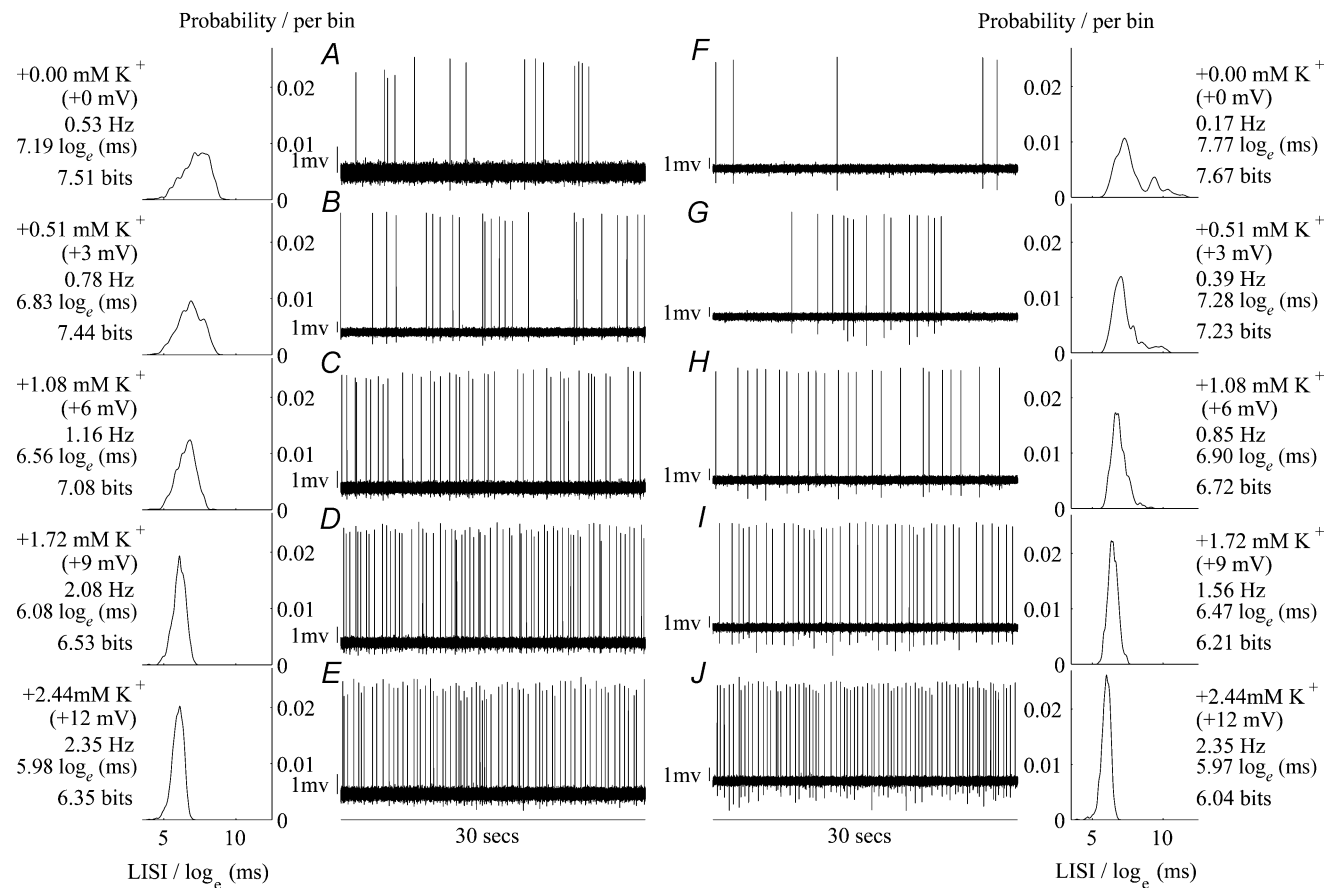


Figure 7. Raising extracellular potassium to depolarize the cells in the suprachiasmatic nucleus affects the distribution of intervals as well the mean spike frequency

The central panels with the waveform traces A–E and F–J show 30 s excerpts of recording from two different cells recorded *in vitro*. Each trace was taken from a 5 min recording that was used to construct the probability mass functions for the log intervals, that are shown to left (for traces A–E) or to the right (for traces F–J) adjacent to the accompanying trace, using a bin width of 0.02 log_e (time). Alongside each probability distribution, the increase in extracellular potassium concentration (in mM), the corresponding estimated depolarization (in mV), mean spike frequency (in Hz), log interval mean (in log_e (ms)) and entropy (in bits) are given. Depolarization causes an increase in mean spike frequency and a decrease in the log interval mean and entropy (see Fig. 8A).

was constructed from 5 min of steady-state recording of which the middle 30 s was used to show an excerpt of the accompanying waveform trace. For both cells, depolarization resulted in an increase in mean spike frequency, and a decrease in the log interval mean. This meant that as the firing rate increased, the position of the log interval histogram shifted to the left. The entropy of log interval distribution decreased as the neurones became more depolarized despite its theoretical independence from mean spike frequency. This is reflected in Fig. 7 by the increasing regularity of spike activity shown in the excerpts of waveform traces and by the reduction in the dispersion of the probability distributions of the log intervals.

While Fig. 8A plots the data for the two example cells, the remaining panels represent the group data for

the mean spike frequency (Fig. 8B), log interval mean (Fig. 8C), and the entropy (Fig. 8D). The group data show similar underlying trends. The estimated extent of depolarization was associated with an increase in mean spike frequency (Fig. 8B) and a reduction in both log interval mean and entropy. Since the positive skew in the mean spike frequencies resulted in a substantial departure from a normal distribution, the data are represented using a box-and-whiskers plot rather than means and standard error bar charts. Spearman's rank coefficient was used to test for statistically significant associations with the estimated extent of depolarization and confirmed a positive trend for mean spike frequency ($r = 0.259$, $P = 0.011$), a weak negative trend for the log interval mean ($r = -0.215$, $P = 0.038$) and a substantially

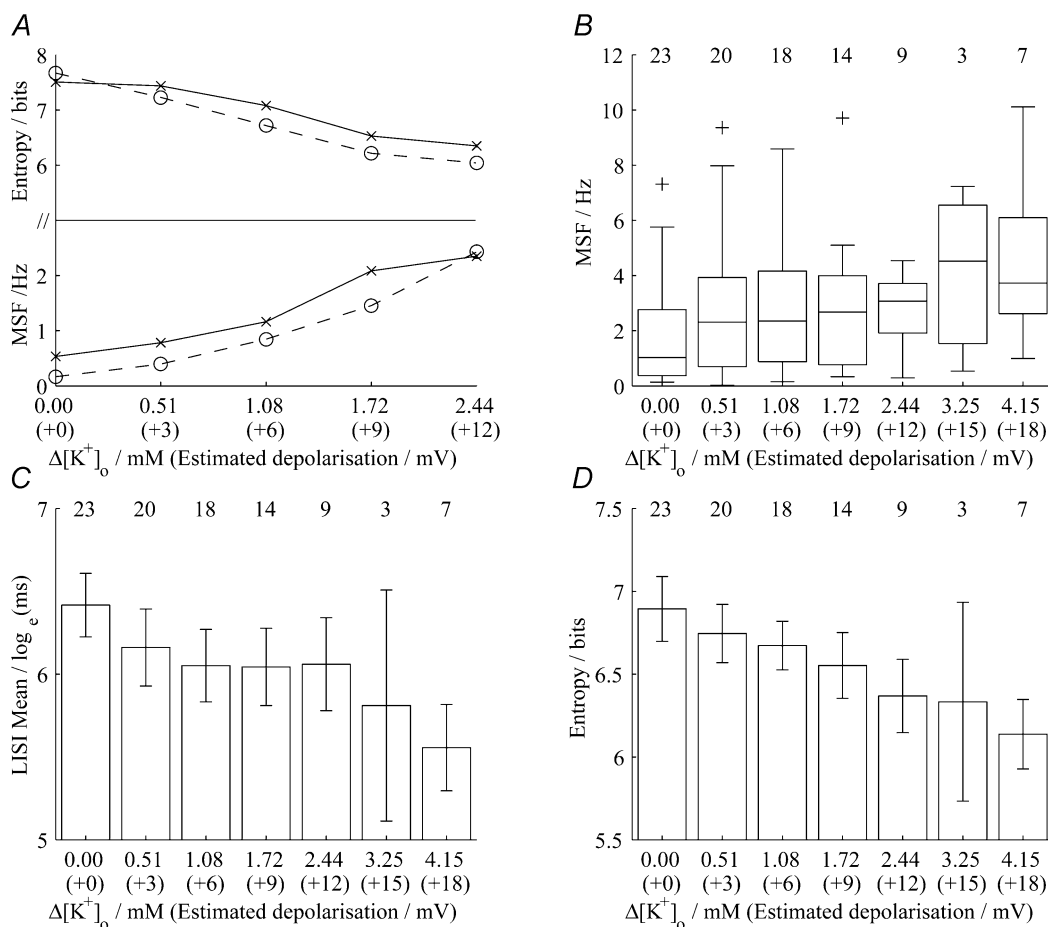


Figure 8. Raising extracellular potassium to depolarize the cells in the suprachiasmatic nucleus reduced the log interval mean and entropy as well as increasing mean spike frequency

A, changes in mean spike frequency (MSF) and entropy for the two cells shown in the previous figure with the continuous line to represent the cell shown in Fig. 7A–E and a dashed line for the neurone represented in Fig. 7F–J. Changes in mean spike frequency for the group data are shown in B using box-and-whiskers plots, with the cell numbers indicated above (see Fig. 1B for an explanation of the box-and-whiskers plot). Mean and standard error bar charts are shown to represent the changes in the log interval mean (LIISI Mean) (C) and entropy (D). Spearman's rank coefficient showed a significant positive trend with respect to depolarization for the mean spike frequency ($r = 0.259$, $P = 0.011$), a weak negative trend for the log interval mean ($r = -0.215$, $P = 0.038$) and a somewhat stronger negative trend for the entropy ($r = -0.296$, $P = 0.004$).

stronger negative trend for the entropy ($r = -0.296$, $P = 0.004$).

Comparisons were made between the neural activity of the 23 cells recorded *in vitro*, before they were subjected to raised extracellular potassium, and the activity recorded *in vivo*. Since the *in vitro* recordings were made only at times that spanned the subjective night-time period, only those 217 recordings made *in vivo* during the subjective night-time were used for the comparison shown in Fig. 9. The Wilcoxon rank sum test showed no significant differences ($z = 0.412$, $P = 0.680$) in mean spike frequency (Fig. 9A). Similarly a two-tailed t test showed no significant differences ($t = -0.298$, $P = 0.766$) in the log interval mean (Fig. 9B). By contrast a similar test showed that the entropy of the log interval distribution (Fig. 9C) was significantly greater *in vivo* than *in vitro* ($t = 5.21$, $P < 0.001$).

Differences between the activity recorded *in vivo* and *in vitro* were investigated with regard to the correlations between mean spike frequency, log interval mean, and entropy after including all the *in vitro* data from cells subjected to raised extracellular potassium. An ANOCOVA (analysis of covariance) test (available in the MathWorks MATLAB 6.1 Statistical Toolbox) was used to test for significant differences in the gradient when comparing the *in vivo* and *in vitro* scatters. There was no significant difference in the trend between the log interval mean plotted against the mean spike frequency (Fig. 9E) when comparing the *in vivo* and *in vitro* groups ($F = 3.11$, $P = 0.079$). However, the slopes of the two groups significantly differed when the entropy of the log interval distribution was plotted against both the log frequency ($F = 15.5$, $P < 0.001$, Fig. 9D) and the log interval mean ($F = 8.41$, $P = 0.004$, Fig. 9F). This means that the

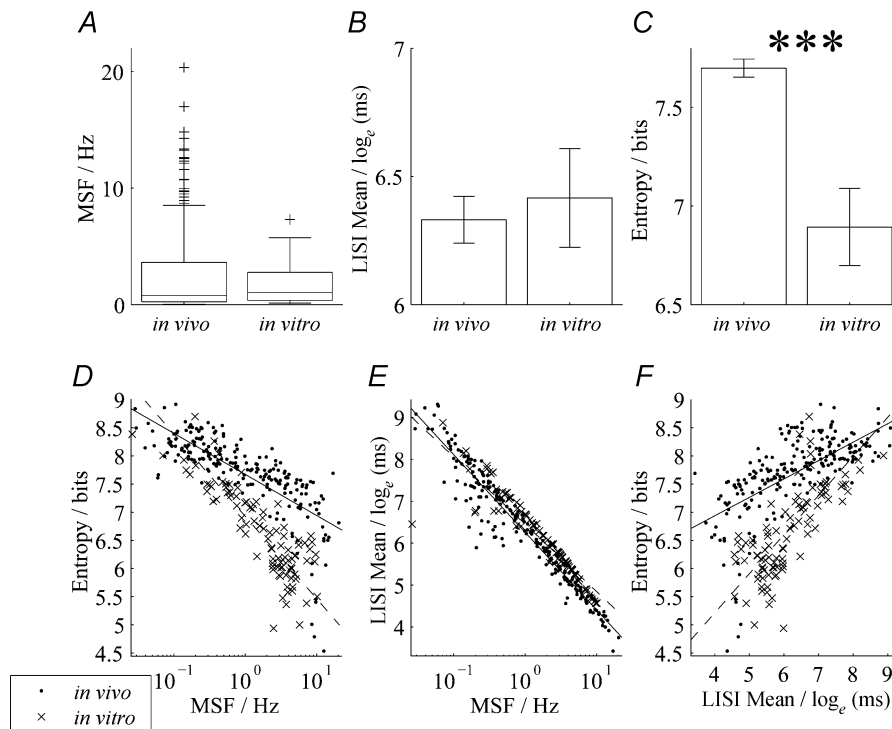


Figure 9. Activity of cells in the suprachiasmatic nucleus recorded *in vivo* is different from that recorded *in vitro*

A–C, comparison of *in vivo* data with the *in vitro* data, without additional depolarization, representing the mean spike frequency (MSF) using a box-and-whiskers plot (A) and showing mean and standard error bar charts to compare the log interval mean (LISI Mean) (B) and entropy (C) for the two groups. An explanation of the box-and-whiskers plot is provided in the legend of Fig. 1. The entropy was significantly greater *in vivo* than *in vitro* ($t = 5.21$, $P < 0.001$). D–F the three measures of activity plotted against each other for the *in vivo* data and the *in vitro* data that included the recordings from depolarized cells. The mean spike frequency is plotted on a log scale in D and E. Scatter points representing *in vivo* data are shown as dots whereas crosses are used to represent *in vitro* recordings. Underlying trends in the *in vivo* data are shown as continuous lines whereas dashed lines are used to represent trends in the *in vitro* data. An ANOCOVA test for differences in the gradients between the *in vitro* and *in vivo* showed no significant difference in the trend between the log mean interval plotted against the mean spike frequency ($F = 3.11$, $P = 0.079$) but differences were shown when plotting the entropy of the log interval distribution against both log frequency ($F = 15.5$, $P < 0.001$) and log interval mean ($F = 8.41$, $P = 0.004$).

entropy was more sensitive to changes in frequency or log interval mean for the cells recorded *in vitro* than for those recorded *in vivo*.

Discussion

Changes in entropy

While there is a daily rhythm of mean spike frequency in the suprachiasmatic nucleus, other aspects of the spike trains may also carry information. The entropy of log intervals was devised as a method to quantify aspects of spike irregularity in a way that avoided having to count spikes over time bins of arbitrary duration (Bhumbra & Dyball, 2004). Using a logarithmic scale for the interspike intervals, the entropy measure is rendered independent of both the mean spike frequency and the units used to quantify time. Cells that show regular firing activity in the suprachiasmatic nucleus are rare (Groos & Hendriks, 1979), and hence any consideration of the irregularity of firing quantified by the log interval entropy is likely to be of physiological interest.

The simplicity of mean spike frequency is its main advantage and it is almost universally used as a measure of activity in suprachiasmatic physiology. However, the diurnal variation of frequencies in Fig. 1 appears to be no more obvious than the rhythm of entropy shown in Fig. 2. A comparison of Figs 1 and 2 suggests that aspects of coding (irregularity in spike activity) in addition to mean spike frequency may also be important in conveying circadian information. Variance measures, such as the standard deviation or the coefficient of variation of intervals (Saeb-Parsy & Dyball, 2003) have been used in the past to quantify the irregularity of cell activity. However, the strong positive skew in the interval histograms of hypothalamic cells means that such variance measures predominantly reflect the extent of the dispersion of very long intervals (Bhumbra & Dyball, 2004) rather than the short intervals that are at least equally likely to be of physiological interest.

Figure 6D shows that, for this group of cells, the log interval entropy was strongly related to the standard deviation of the log interspike interval. However the advantage of the use of entropy rather than for example the standard deviation or variance of the log interspike intervals is that entropy is sensitive to the shape and modality as well as the dispersion of the interval distributions. Certain groups of cells within the suprachiasmatic nucleus are known to show bimodal interval distributions (Saeb-Parsy & Dyball, 2003). The advantage of the log interval entropy over the standard deviation or variance of the log interspike intervals is that it is a single measure that can reflect a change from a unimodal to a bimodal distribution and be equally valid in both situations if the modality should change.

The logarithmic transformation of the interspike intervals renders the entropy very sensitive to the presence of very short intervals. Any occurrence of doublet or couplet spike motifs may not be detected if overall mean spike frequencies were considered alone (Bhumbra & Dyball, 2004). The entropy measure may thus be more closely related to influences on neural communication, for example an increase in free intracellular calcium ion concentration or release of transmitter from synaptic terminals, than mean spike frequency in those cells with slow overall firing rates such as those of the suprachiasmatic nucleus. It is not possible to measure transmitter release from the cells we recorded, but in the supraoptic nucleus the magnocellular neurones show greater efficiency in neuropeptide release for a given number of spikes with more patterned motifs of activity (Dutton & Dyball, 1979). It has also been known for some time that a brief series of short intervals can influence the excitability of some hypothalamic cells (Dyball & McKenzie, 2000) and we have recently shown that similar effects occur in cells of the suprachiasmatic nucleus (Dyball & Inyushkin, 2005).

Urethane was used throughout the experiments *in vivo* and the level of anaesthesia remained constant. There is no evidence to suggest that time under urethane anaesthesia has a systematic affect on the firing of suprachiasmatic cells (Saeb-Parsy & Dyball, 2003). It is thus unlikely that the anaesthetic imposed any artefactual rhythm. It may have attenuated the extent of the rhythm but despite its possible influence, application of the Monte-Carlo algorithm to the log interval entropy showed a high level of significance in rhythmic activity of suprachiasmatic cells. Another possible factor that may have affected the rhythm activity was the level of ambient light during the experiments. The animals needed to be exposed to light during the surgery and placement of electrodes. To avoid variations in the time of light exposure in different experiments, we maintained constant illumination throughout the recording that may have attenuated but could not have imposed a rhythm (see methods).

Recordings were made from the suprachiasmatic nucleus from the ventral side to avoid the inaccuracies of electrode placement that might have arisen using a dorsal approach. Although the profiles of the changes in log interval entropy were similar, the rhythmic activity of cells in the central region of the suprachiasmatic nucleus was more obvious than that in the peripheral zone. Figure 3 illustrates that the changes in activity over the light-dark transition were more marked in the central region than in the peripheral zone. Although there is no defined boundary for the cells that constitute the suprachiasmatic nucleus, the less obvious rhythm seen in the peripheral zone is likely to reflect a dilutional effect because of the inclusion of cells outside the nucleus that attenuated any oscillatory changes. Similarities in the profiles of the

rhythm suggest some degree of common function for the two areas, and any consideration of the combined data for the log interval entropy is likely to be representative of the global activity seen throughout the nucleus (see Methods).

While classification of cell type by histologically defined location did not show substantial differences in rhythmic activity, Fig. 4 suggests that neurones with an outward projection to the region of the arcuate nucleus show a rhythm in activity that appears to be distinctly biphasic whereas those cells without such a connection showed a single peak. Some of the stimulated axons may have projected beyond the arcuate nucleus but all must have projected outside the suprachiasmatic nucleus. The appearance of a biphasic rhythm in cells that send their axons to other hypothalamic brain areas has been suggested earlier (Saeb-Parsy & Dyball, 2003). Antidromically activated cells may have shown 12 h rhythms either as a result of a halving of the period in oscillation due to intrinsic ultradian rhythmicity, or because of the presence of two populations of cells with a period of 24 h but 12 h out of phase with each other.

To investigate the possibility of ultradian rhythmicity, it would be useful to undertake recordings of antidromically identified single units *in vivo* for periods greater than 24 h. Long-term recordings *in vitro* (Bos & Mirmiran, 1990; Welsh *et al.* 1995; Herzog *et al.* 1997; Liu *et al.* 1997; Herzog *et al.* 1998; Honma *et al.* 1998; Liu & Reppert, 2000) have shown rhythmic single unit activity with a period of 24 h rather than 12 h. However, periodicity of approximately 12 h has been suggested by the expression of adenylyl cyclase (Cagampang *et al.* 1998a), protein kinase C (Cagampang *et al.* 1998b), and the vasoactive intestinal peptide 2 receptor (Cagampang *et al.* 1998c). Levels of cAMP in the suprachiasmatic nucleus *in vitro* appear to show biphasic rhythmicity (Prosser & Gillete, 1991), suggesting that certain aspects of the circadian clock are likely to show a functional ultradian periodicity of approximately 12 h.

The cells that sent their axons towards the region of arcuate nucleus showed two distinctive peaks in entropy during the mid-light and mid-dark periods and two troughs in the transition periods. It is of particular interest that the mean spike frequency of cells with outward projections to other hypothalamic areas, with two troughs in the mid-light and mid-dark periods and two peaks in the transition periods (Saeb-Parsy & Dyball, 2003), show an opposite pattern. Figure 6C illustrates the positive relationship between the irregularity of cell firing and the resting firing state by plotting the log interval entropy against the mean. An inverse relationship between mean spike frequency and the coefficient of variation has been shown previously (Saeb-Parsy & Dyball, 2003), but the use of the coefficient of variation is limited as a physiological measure of irregularity since it is strongly associated with the skewness of the interval histogram that is distorted by

the presence of very long intervals (Bhumbra & Dyball, 2004).

Rates and irregularity

Aspects of activity in addition to spike frequency, for example the irregularity of firing, may be important in conveying information (Rieke *et al.* 1999). The log interval mean and entropy have been used previously to characterize the central position and variability of the log interspike interval histogram for cells recorded in the supraoptic nucleus (Bhumbra & Dyball, 2004). Since the interspike interval histogram uniquely determines the mean spike frequency, the log interval mean and entropy might be expected to be related to the spike rate in a way that reflects the association between the excitable state of the neurone and the irregularity of its activity. However, as shown by the dispersion of the scatter in Fig. 6B, the mean spike frequency is not only a function of the reciprocal of the antilog of the log interval mean (μ) because the mean interval is also affected by the logarithmic standard deviation (σ). The expected value $E(w)$ of a lognormal probability density function $f(w)$ for the variable w , whose natural logarithm x of mean μ and variance σ^2 , is given by $E(w) = e^{\mu + \sigma^2/2}$ (Aitchison & Brown, 1963). If w is lognormally distributed, then the probability density function $f(x)$ of its natural logarithm x would be given by a Gaussian function $\mathcal{N}(\mu, \sigma^2)$. Whereas eqn (1) expresses a discrete entropy with respect to a summation, it is possible to express a continuous counterpart, or differential entropy, using an integral. The differential entropy $s(X)$ of a normal probability density function $\mathcal{N}(\mu, \sigma^2)$ can be expressed with respect to the variance σ^2 by expanding the integration terms (Cover & Thomas, 1991):

$$s(X) = - \int_{-\infty}^{\infty} \mathcal{N}(\mu, \sigma^2) \log_2 \mathcal{N}(\mu, \sigma^2) dx \quad (4)$$

$$= \frac{1}{2} \log_2 2\pi e \sigma^2 \quad (5)$$

For a small bin width δx , the discrete entropy $S(X)$ and differential entropy $s(X)$ can be interrelated (Cover & Thomas, 1991):

$$S(X) = s(X) - \lim_{\delta x \rightarrow 0} \delta x \quad (6)$$

$$= \frac{1}{2} \log_2 2\pi e \sigma^2 - \lim_{\delta x \rightarrow 0} \delta x \quad (7)$$

$$= \lim_{\delta x \rightarrow 0} \log_2 \left(\frac{\sqrt{2\pi e \sigma^2}}{\delta x} \right) \quad (8)$$

$$= \log_2(\sigma) + \lim_{\delta x \rightarrow 0} \log_2 \left(\frac{\sqrt{2\pi e}}{\delta x} \right) \quad (9)$$

Hence if all the log interval histograms conformed to a normal distribution, the relationship between $S(X)$ plotted against $\log_2\sigma$ would be linear with a gradient of one and an intercept of $\log_2(\sqrt{2\pi e}/\delta x)$ (≈ 7.69 bits). For the data obtained *in vivo* the graphical relationship was strongly linear as shown in Fig. 6D, and the entropy $S(X)$ could be related to the standard deviation σ using linear regression: $S(X) = 0.905 \log_2(\sigma) + 7.57$. The upper limit for the 99.9% confidence for the slope was 0.940 and the intercept, 7.59. A Gaussian model for the log interval histogram would predict a slope of 1 and an intercept of 7.69 and would thus over-estimate the entropy seen for the observed data *in vivo*. Since a Gaussian function maximizes the entropy of a probability density function given a fixed variance (Jaynes, 2003), it is perhaps not surprising that an entropy estimate from the variance based on the assumption of normality would be an over-estimate. Despite the discrepancy, there is a strong linear relationship between the log interval standard deviation and entropy, showing that the log variance is a measure that reflects the coding capacity of the cell reasonably well. However, unlike standard deviations, entropies have the distinct advantage in that they are not restricted to second order statistics. Entropy measures are thus sensitive to more features of a probability distribution than variances. Since the activity of the cells could not be represented using a Gaussian model, entropies are likely to reflect aspects of coding not described by variances.

A 99.9% confidence interval from 0.869 to 0.940 for the slope of $S(X)$ plotted against $\log_2\sigma$ does not include the value of 1 and thus shows that the log interval histograms for the cells were not simply non-Gaussian, but that the departure from normality increased for the more irregularly firing cells. Because the entropy was negatively correlated with the mean spike frequency, this departure from normality in the interval distribution is likely to be greater for the slower rather than faster firing cells. For example, the firing of a slow firing cell may give rise to a bimodal lognormal interval histogram as a result of doublet or triplet spike motifs that are characteristic of the activity of some types of hypothalamic cell, such as those in the perinuclear zone of the supraoptic nucleus (Bhumbra & Dyball, 2004). It is of particular interest that two spikes in close temporal proximity carry far more than double the information conveyed by a single spike (Brenner *et al.* 2000) and such aspects of activity are neglected when considering frequencies alone.

Although Fig. 6C suggests that the relationship between the log interval entropy and mean is strong, it is not always linear. The entropy is highly sensitive to changes in the log interval mean when the mean value is very

low and reaches a plateau as the mean increases beyond approximately $7 \log_e$ milliseconds. Using the log interval entropy, it is possible to quantify the balance between stochastic factors, such as the Poisson nature of synaptic inputs, and deterministic factors, such as the profile of the after-polarization potential and depolarizing after-potential (Bhumbra *et al.* 2004a). For the cells with a higher log interval mean, the log interval entropy approximates to the value that corresponds to the entropy of a Poisson process: 7.95 bits per event, independent of frequency (Bhumbra & Dyball, 2004). This reflects the stochastic nature of the synaptic inputs that are more influential on such recordings, whereas the dramatic reduction in the entropy for cell recordings with a reduced log interval mean must result from an increased deterministic influence of the channel membrane properties on spike activity. This may be comparable to the situation where motor neurones fire relatively deterministically at high rates, whereas at low rates the time of firing is more susceptible to synaptic noise (Matthews, 1996). Figure 2A and B shows that the lowest values for entropy were clustered over the day–night transition suggesting that the membrane properties of clock cells were altered transiently during this period. Since the spike rates are not affected by any variability in the interval distribution, spike frequency alone would be inadequate to detect such potentially physiologically important changes in rhythmic activity.

Zeitgeber coding by depolarization

The purpose of the experiments involving depolarization *in vitro* was to determine whether the differences seen *in vivo* at different times of day might have been due to depolarization. The statistical correlations between the log interval entropy and both mean spike frequency (Fig. 9D) and log interval mean (Fig. 9F) were different for the *in vivo* and *in vitro* preparations. Thus measures in addition to firing rate are worthwhile and may be necessary to discern differences between the spike activity in different situations (Bhumbra & Dyball, 2004). We focused on the activity during the subjective night time because previous work (Saeb-Parsy & Dyball, 2003) suggested that the cells of suprachiasmatic nucleus showed greater homogeneity in activity during the dark period. Differences were seen during the night. Recordings in the daytime might also have shown similar differences but would not have altered the argument, specifically that measures based on the shape and dispersion of log intervals can quantify differences that are not obvious from frequency measures.

The *in vitro* data showed that depolarization not only increased the mean spike frequency but decreased the log interval mean and entropy. We expected that the deafferentation during the preparation of the hypothalamic slices would distort the spike activity in a way that reduces the extent of coding (Bhumbra & Dyball,

2004). Figure 9C shows that during the subjective night the log interval entropy was significantly lower *in vitro* than *in vivo*. This is likely to be a consequence of severing the neural inputs. However, despite the differences in entropy there were no significant differences in the mean spike frequencies and log interval means between the *in vivo* and *in vitro* groups, and the negative correlation between the two measures did not significantly differ in their correlation for the two preparations, as shown in Fig. 9E.

Depolarization of neurones in the suprachiasmatic nucleus *in vitro* caused an increase in mean spike frequency and a decrease in the log interval mean and entropy. However, Fig. 9D and F showed that the nature of the interdependence between the entropy and the other two measures was not the same *in vitro* as it was *in vivo*. The differences in the correlations cannot be simply attributed to the reduced entropy seen *in vitro* since the significance applies to the slopes rather than the intercepts. In other words, two crossing lines fitted the scatters in a way that was significantly more representative of the data than two parallel lines. Both types of fit would have accommodated any differences in the mean entropy for the two groups. The greater gradient *in vitro* of the entropy against both mean spike frequency and the log interval mean suggests a greater importance of deterministic factors (such as the profile of the afterhyperpolarization potential) relative to stochastic influences (such as the activity of inputs) in affecting neuronal firing in the hypothalamic slice as compared with the intact animal.

Both the *in vivo* and *in vitro* data show negative correlations for the entropy plotted against the mean spike frequency but the steeper line *in vitro* (Fig. 9D) suggests that there is a relative decrease in afferent information consistent with the loss of inputs in the slice preparation. It is thus possible that the diurnal changes in both mean spike frequency and the irregularity of activity seen *in vivo* may result from daily changes in the depolarized states of cells of the suprachiasmatic nucleus. Diurnal changes in intracellular calcium levels in individual neurones (Ikeda *et al.* 2003) support the contribution of calcium currents to the generation of spontaneous oscillations in membrane potential. Differences in the behaviour of the L-type calcium current between the day and night (Pennartz *et al.* 2002) suggest that intrinsic ionic currents may be important in circadian function. The presence of a number of different calcium channel subtypes and the modulatory effects of calcium on ion-gated potassium channels has been shown in cells of the suprachiasmatic nucleus (Cloues & Sather, 2003), suggesting that the profile of the afterhyperpolarization potential may be important in circadian function. However, the afterhyperpolarization potential has a far greater effect on the variability of firing than on mean spike frequency in slow firing cells (Matthews, 1996), such as those in the hypothalamus. Among a group of neurones such as those in the suprachiasmatic

nucleus, absolute differences in firing rates are more obvious among faster firing cells than slower firing cells and such differences may disguise substantial differences in more subtle aspects of neural activity. The physiological importance of membrane channels in circadian rhythmicity may thus be reflected more effectively by considering changes in irregularity of firing rather than simply averaging the firing rates of cells of a number of different subtypes.

It may be misleading to regard differences in the activities in cells of the suprachiasmatic nucleus purely as noise. Many established methods of profiling the changes in spontaneous activity over the day–night cycle are based on averages of mean spike counts in a way that does not quantify the irregularity of firing. Moreover, such techniques do not consider any changes in the variability of cell activity within the nucleus as a possible manifestation of rhythm. We present data that show that the irregularity of spike activity, as quantified by the log interval entropy, shows at least as clear a rhythm as mean spike frequency. Rhythmic changes in entropy of cells in the central region of the suprachiasmatic nucleus is convincing, with a higher level of significance than that seen in the peripheral zone. By comparing the activities of cells with and without projections towards the region of the arcuate nucleus, we show that antidromically identified cell types exhibit differences in activities that can be readily seen using the entropy of the log intervals. By depolarizing cells of the suprachiasmatic nucleus, we show that the mean spike frequency increases and the log interval entropy decreases in a way that might be expected after partial deafferentation that would reduce the relative influence of synaptic inputs. Our results show that rhythmic activity may be measured by the irregularity of firing as well as average spike rates.

Appendix

The extent of the increase in extracellular potassium was used to estimate the degree of depolarization, based on their interrelation given by the Nernst equation:

$$E = \frac{RT}{F} \log_e \left(\frac{[K^+]_o}{[K^+]_i} \right) \quad (10)$$

where E is an estimate of the membrane potential based only on intracellular and extracellular potassium concentrations, R is the ideal gas constant ($8.3143 \text{ J mol}^{-1} \text{ K}^{-1}$), T is the absolute temperature (306 K), F is Faraday's constant (96485 C mol^{-1}), $[K^+]_o$ is the concentration of potassium in the aCSF (4.24 mM) and $[K^+]_i$ is the concentration inside the cell.

A value for E could not be determined since the intracellular concentration of potassium $[K^+]_i$ was unknown. However, changes in E , due to a depolarization ΔE as a result of increasing the extracellular potassium concentration $[K^+]_o$ by $\Delta [K^+]_o$, could be estimated using

a derivation based on the assumption that the internal potassium concentration $[K^+]_i$ remained constant:

$$E + \Delta E = \frac{RT}{F} \log_e \left(\frac{[K^+]_o + \Delta[K^+]_o}{[K^+]_i} \right) \quad (11)$$

The extent of depolarization ΔE can thus be expressed by subtracting eqn (10) from eqn (11):

$$E + \Delta E - E = \frac{RT}{F} \log_e \left(\frac{[K^+]_o + \Delta[K^+]_o}{[K^+]_i} \right) - \frac{RT}{F} \log_e \left(\frac{[K^+]_o}{[K^+]_i} \right) \quad (12)$$

$$\Delta E = \frac{RT}{F} \left[\log_e \left(\frac{[K^+]_o + \Delta[K^+]_o}{[K^+]_i} \right) + \log_e \left(\frac{[K^+]_i}{[K^+]_o} \right) \right] \quad (13)$$

The right hand expression could be simplified by expanding the logarithmic terms:

$$\Delta E = \frac{RT}{F} \left[\log_e ([K^+]_o + \Delta[K^+]_o) - \log_e [K^+]_i + \log_e [K^+]_i - \log_e [K^+]_o \right] \quad (14)$$

$$= \frac{RT}{F} \left[\log_e ([K^+]_o + \Delta[K^+]_o) + \log_e [K^+]_o \right] \quad (15)$$

$$= \frac{RT}{F} \log_e \left(\frac{[K^+]_o + \Delta[K^+]_o}{[K^+]_o} \right) \quad (16)$$

$$= \frac{RT}{F} \log_e \left(1 + \frac{\Delta[K^+]_o}{[K^+]_o} \right) \quad (17)$$

The right hand expression shows that the change in the membrane potential ΔE is independent of the intracellular concentration of potassium $[K^+]_i$. By rearranging the equation, it is possible to express the change in extracellular potassium $\Delta[K^+]_o$ that would be required to produce a desired depolarization ΔE with respect to the initial concentration $[K^+]_o$:

$$\log_e \left(1 + \frac{\Delta[K^+]_o}{[K^+]_o} \right) = \frac{F \Delta E}{RT} \quad (18)$$

$$1 + \frac{\Delta[K^+]_o}{[K^+]_o} = e^{F \Delta E / RT} \quad (19)$$

$$\frac{\Delta[K^+]_o}{[K^+]_o} = e^{F \Delta E / RT} - 1 \quad (20)$$

$$\therefore \Delta[K^+]_o = [K^+]_o (e^{F \Delta E / RT} - 1) \quad (21)$$

It was thus possible calculate the required increase in extracellular potassium concentration $\Delta[K^+]_o$ to give an increase in the estimated extent of depolarization ΔE .

References

- Aitchison J & Brown J (1963). *The Lognormal Distribution*. Cambridge University Press, Cambridge, UK.
- Bhumbra G & Dyball R (2004). Measuring spike coding in the supraoptic nucleus. *J Physiol* **555**, 281–296.
- Bhumbra G, Inyushkin A & Dyball R (2004a). Assessment of spike activity in the supraoptic nucleus. *J Neuroendocrinol* **16**, 390–397.
- Bhumbra G, Saeb-Parsy K & Dyball R (2004b). Daily rhythms of spike coding in the suprachiasmatic nucleus. *J Physiol* **555.P**, C38.
- Bos N & Mirmiran M (1990). Circadian rhythms in spontaneous neuronal discharge of the cultured suprachiasmatic nucleus. *Brain Res* **511**, 158–162.
- Bouskila Y & Dudek F (1993). Neuronal synchronization without calcium-dependent synaptic transmission in the hypothalamus. *Proc Natl Acad Sci U S A* **90**, 3207–3210.
- Brenner N, Strong S, Koberle K, Bialek W & de Ruyter Van Steveninck R (2000). Synergy in a neural code. *Neural Comp* **12**, 1231–1552.
- Cagampang F, Antoni F, Smith S & Piggins H (1998a). Circadian changes of type II adenylyl cyclase mRNA in the rat suprachiasmatic nuclei. *Mol Brain Res* **810**, 279–282.
- Cagampang F, Rattray M, Campbell I, Powell J & Coen C (1998b). Variation in the expression of the mRNA for protein kinase c isoforms in the rat suprachiasmatic nuclei, caudate putamen and cerebral cortex. *Mol Brain Res* **53**, 277–284.
- Cagampang F, Sheward W, Harmar A, Piggins H & Coen C (1998c). Circadian changes in the expression of vasoactive intestinal peptide-2-receptor mRNA in the rat suprachiasmatic nuclei. *Mol Brain Res* **54**, 108–112.
- Cloues R & Sather W (2003). Afterhyperpolarization regulates firing rate in neurons of the suprachiasmatic nucleus. *J Neurosci* **23**, 1593–1604.
- Cover T & Thomas J (1991). *Elements of Information Theory*. John Wiley, New York.
- Cui L-N, Saeb-Parsy K & Dyball R (1997). Neurons in the supraoptic nucleus of the rat are regulated by a projection from the suprachiasmatic nucleus. *J Physiol* **502**, 149–159.
- Dutton A & Dyball R (1979). Phasic firing enhances vasopressin release from the rat neurohypophysis. *J Physiol* **290**, 433–440.
- Dyball R & Bhumbra G (2003). Digital spike discrimination combining size & shape elements. *J Physiol* **547.P**, D9 (abstract).
- Dyball REJ & Inyushkin AN (2005). Burst stimulation alters the excitability of hypothalamic axons. *J Physiol* **563.P**, C54 (abstract).
- Dyball REJ & McKenzie DN (2000). Synchronised clusters of action potentials can increase or decrease the excitability of the axons of magnocellular hypothalamic neurosecretory cells. *J Neuroendocrinol* **12**, 729–735.
- Gerstein G & Mandelbrot B (1964). Random walk models for the spike activity of a single neuron. *Biophys J* **4**, 41–68.
- Green D & Gillette R (1982). Circadian rhythm of firing rate recorded from single cells in the rat suprachiasmatic brain slices. *Brain Res* **245**, 198–200.
- Groos G & Hendriks J (1979). Circadian rhythms in electrical discharge of rat suprachiasmatic neurons recorded *in vitro*. *Experientia* **35**, 1597–1598.

- Groos G & Hendriks J (1982). Circadian rhythms in electrical discharge of rat suprachiasmatic neurons recorded *in vitro*. *Neurosci Lett* **34**, 283–288.
- Herzog E, Geusz M, Khalsa S, Straume M & Block G (1997). Circadian rhythms in mouse suprachiasmatic nucleus explants on multimicroelectrode plates. *Brain Res* **757**, 285–290.
- Herzog E, Takahashi J & Block G (1998). Clock controls circadian period in isolated suprachiasmatic nucleus neurons. *Nature Neurosci* **1**, 708–713.
- Honma S, Shirakawa T, Katsuno Y, Namihara M & Honma K (1998). Circadian periods of single suprachiasmatic neurons in rats. *Neurosci Lett* **250**, 157–160.
- Ikeda M, Sugiyama T, Wallace C, Gompf H, Yoshioka T, Miyawaki A & Allen C (2003). Circadian dynamics of cytosolic and nuclear Ca^{2+} in single suprachiasmatic nucleus neurons. *Neuron* **38**, 253–263.
- Inouye S-I & Kawamura H (1979). Persistence of circadian rhythmicity in a mammalian hypothalamic ‘island’ containing the suprachiasmatic nucleus. *Proc Natl Acad Sci U S A* **76**, 5962–5966.
- Jaynes E (2003). *Probability Theory: The Logic of Science*. Cambridge University Press, Cambridge, UK.
- Leak RK, Card JP & Moore RY (1999). Suprachiasmatic pacemaker organization analyzed by viral transsynaptic transport. *Brain Res* **819**, 23–32.
- Leng G & Dyball R (1985). Functional identification of magnocellular neuroendocrine neurones. In *Neuroendocrine Research Methods*, ed. Greenstein, B, Taylor & Francis, London.
- Liu C & Reppert S (2000). GABA synchronizes clock cells within the suprachiasmatic circadian clock. *Neuron* **25**, 123–128.
- Liu C, Weaver D, Jin X, Shearman L, Pieschi R, Gribkoff V & Reppert S (1997). Molecular dissection of two distinct actions of melatonin on the suprachiasmatic circadian clock. *Neuron* **19**, 91–102.
- Matthews P (1996). Relationship of firing intervals of human motor units to the trajectory of post-spike after-hyperpolarization and synaptic noise. *J Physiol* **492**, 597–628.
- Meijer J, Schaap J, Watanabe K & Albus H (1997). Multiunit activity recordings in the suprachiasmatic nuclei: *In vivo* versus *in vitro* models. *Brain Res* **753**, 322–327.
- Moore RY & Eichler VB (1972). Loss of circadian corticosterone rhythm following suprachiasmatic nucleus lesions in the rat. *Brain Res* **42**, 201–206.
- Pennartz C, de Jeu M, Bos N, Schaap J & Geurtsen A (2002). Diurnal modulation of pacemaker potentials and calcium current in the mammalian circadian clock. *Nature* **416**, 286–290.
- Prosser R & Gillette M (1991). Cyclic changes in cAMP concentration and phosphodiesterase activity in a mammalian circadian clock studied *in vitro*. *Brain Res* **568**, 185–192.
- Purves D, Augustine G, Fitzpatrick D, Katz L, LaMantia A-S, McNamara J & Williams S (2001). *Neuroscience*. Sinauer Associates Inc., Sunderland, MA, USA.
- Rieke F, Warland D, de Ruyter Van Steveninck R & Bialek W (1999). *Spikes: Exploring The Neural Code*. The MIT Press, Cambridge, MA, USA.
- Saeb-Parsy K & Dyball R (2003). Defined cell groups in the rat suprachiasmatic nucleus have different day/night rhythms of single-unit activity *in vivo*. *J Biol Rhythms* **18**, 26–42.
- Saeb-Parsy K, Lombardelli S, Khan F, McDowall K, Au-Yong I & Dyball R (2000). Neural connections of hypothalamic neuroendocrine nuclei in the rat. *J Neuroendocrinol* **12**, 635–648.
- Shannon C & Weaver W (1949). *The Mathematical Theory of Communication*. University of Illinois Press, Urbana.
- Shibata S, Oomura Y, Kita H & Hattori K (1982). Circadian rhythmic changes in neuronal activity in the suprachiasmatic nucleus of the rat hypothalamic slice. *Brain Res* **302**, 154–158.
- Stephan FK & Zucker I (1972). Circadian rhythms in drinking behaviour and locomotor activity of rats are eliminated by hypothalamic lesions. *Proc Natl Acad Sci U S A* **69**, 2625–2641.
- Wadsworth H (1990). *Handbook of Statistical Methods for Engineers and Scientists*. McGraw-Hill, New York.
- Welsh D, Logothetis D, Meister M & Reppert S (1995). Individual neurons dissociated from rat suprachiasmatic nucleus express independently phased circadian firing rhythms. *Neuron* **14**, 697–706.

Acknowledgements

This work was supported by the Medical Research Council (UK), Engineering and Physical Sciences Research Council (UK), Merck, Sharp, and Dohme (UK), and the James Baird Fund. We are extremely grateful to S. A. Edgley from the University of Cambridge for his assistance in the preparation of this manuscript.